Green Emission to Probe Photoinduced Charging Events in ZnO−Au Nanoparticles. Charge Distribution and Fermi-Level Equilibration†

Vaidyanathan Subramanian,‡,§ Eduardo E. Wolf,§ and Prashant V. Kamat*,‡

Radiation Laboratory and Department of Chemical Engineering, University of Notre Dame, Notre Dame, Indiana 46556-0579

Received: November 20, 2002; In Final Form: January 24, 2003

Photoinduced electron accumulation in ZnO nanoparticles results in the bleaching of the exciton band as well as quenching of green emission. In the absence of an electron scavenger, photogenerated electrons are stored near the conduction band edge and promote charge recombination via a nonradiative process. By exposing the UV-irradiated ZnO suspension to an electron acceptor (O_2 or thionine dye) the stored electrons are discharged and the original excitonic band and the visible emission are restored. Titration of electrons stored in ZnO nanoparticles with an electron acceptor, thionine dye, shows a linear relationship between stored electrons and the emission quenching. When gold nanoparticles are added to pre-UV-irradiated ZnO colloids, only partial recovery of the emission is seen. Pt nanoparticles on the other hand caused almost complete recovery of the quenched emission as the electrons are discharged into the solution. The charge distribution between UV-irradiated ZnO and gold nanoparticles results in equilibration of the Fermi level. Furthermore, the transfer of electrons to the metal nanocore followed by equilibration continues until the Fermi level reaches close to the conduction band edge of ZnO. Basic understanding of the interaction between the semiconductor and metal layers leading to Fermi-level equilibration is important for evaluating the role of noble metals in photocatalytic reactions.

Introduction

A major limitation of achieving high photocatalytic efficiency in semiconductor nanoparticle systems is the quick recombination of charge carriers.[1,2] Efforts have been made by several research groups to overcome this limitation by developing semiconductor−semiconductor and semiconductor−metal type composite nanoclusters.[3−9] For example, the efficiency of a photocatalytic reaction (e.g., water splitting process) can be greatly improved by depositing noble metals on semiconductor nanoparticles. (See, for example, refs 7−18.) Improvement in the photocatalytic performance is achieved by incorporating metal ions into semiconductor nanostructures using ion-impregnation or chemical doping procedures.[19−22]

In our earlier work[23] we have shown that the photoelectrochemical performance of nanostructured TiO_2 films can be improved by coupling them with noble metal nanoparticles. This observation also parallels the studies of Nakato and coworkers[17,24] who reported an enhancement in the photovoltage by deposition of metal islands on single-crystal semiconductors. Whereas the deposition of metal nanoparticles improves both charge separation as well as interfacial charge transfer kinetics, the mechanism responsible for such an improvement is yet to be understood fully on the nanoscale. Unlike bulk films, metal nanoparticles exhibit an unusual property of quantized double layer charging effects.[25] Electrochemical[26,27] and photochemical[28,29] experiments have shown that the gold nanoparticles capped with organic molecules exhibit unusual redox activity by readily accepting electrons from a suitable donor or an electrode. If such metal particles come in contact with a charged semiconductor nanostructure or nanoparticle, they can equilibrate and undergo Fermi-level equilibration (Scheme 1). Often such charge equilibration between the semiconductor and metal nanostructures in contact drives the Fermi level close to the conduction band edge of the semiconductor. Using this hypothesis it has been possible to understand the increase in the photovoltage of TiO_2−Au films[23,30] and charging effects in ZnO−metal colloids.[28]

SCHEME 1: Charge Distribution in Semiconductor−Metal Composite System Leads to Fermi-Level Equilibration

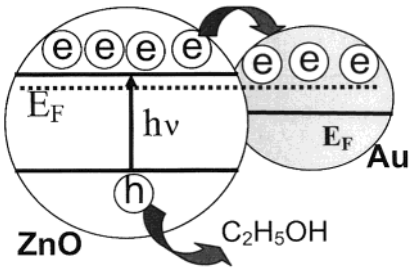

By employing ZnO emission as a probe we have now investigated the charge distribution between metal and semiconductor nanostructures and their Fermi-level equilibration. ZnO is a large band gap semiconductor (E_g = 3.2 eV) with band energies similar to that of TiO_2. Its size quantization properties have been investigated from the dependence of absorption and emission spectra on the size of the particle.[31−34] The green emission arising from the oxygen vacancies is sensitive to the molecular species (e.g., iodide or phenols) present at the interface.[34,35] By making use of this property, nanostructured ZnO films have been successfully employed in

† Part of the special issue "Arnim Henglein Festschrift".

* E-mail: pkamat@nd.edu, or http://www.nd.edu/~pkamat).
‡ Notre Dame Radiation Laboratory.
§ Department of Chemical Engineering (Wolf.1@nd.edu).

10.1021/jp0275037 CCC: $25.00
Published on Web 03/15/2003

simultaneous sensing and degradation of toxic pollutants.[35] Moreover, deposition of a metal such as silver can also influence its emission properties.[36] It is also interesting to note that oxide semiconductor colloids (TiO_2, WO_3, and ZnO) are capable of undergoing charge storage under UV-irradiation. Trapping of electrons in these colloids is accompanied by absorption shift in the band edge or appearance of new absorption in the red-infrared region. The shift in the band edge caused by electron accumulation has been studied by spectroelectrochemical[37,38] and photochemical[28] methods.

We now report a simple and sensitive approach that makes use of an emission property for probing electron storage in ZnO nanoparticles. The results that describe photoinduced charge distribution and Fermi-level equilibration events in ZnO−metal nanocomposite particles are presented here.

Experimental Section

Preparation of ZnO Colloids. ZnO colloids were prepared as per an earlier reported procedure.[33,34] An amount of 0.1 M zinc acetate dihydrate (2.19 g) was added to 100 mL of ethanol and refluxed for 2 h followed by gradual cooling to room temperature with a drying tube attached at the end (in order to prevent exposure to ambient moisture). The precursor solution was (0.1 M) stored in the desiccator and remained stable for weeks. When required for experimentation, small batches of colloidal suspension were prepared by hydrolysis using LiOH powder. This simplified procedure enabled us to maintain reproducibility of sample preparation. In a typical procedure, lithium hydroxide (22 mg) was added directly to 5 mL of the precursor solution, diluted to 25 mL with ethanol, and sonicated at 273 K for 15 min. The ZnO suspension (0.02 M) prepared in this manner was transparent and stable when kept in a sealed flask. The ZnO suspension was further diluted to 4 mM and allowed to stabilize for 4 h before employing it in UV-irradiation experiments. (Note that in early times (1−2 h) the ZnO particles grew in size and caused a continuous shift in the absorption and emission bands. Such a particle growth makes the probing of absorption and emission spectra difficult during this initial growth period. Allowing it to stabilize for ∼2 h minimized this undesired effect on the absorption and emission changes and gave reproducible results for the experiments described in this study.

Preparation of Metal-Capped Semiconductor Composites. To prepare stable metal colloid solution in ethanol one needs to employ a stabilizer. We employed preformed TiO_2 colloids as the support core to deposit the desired metal capping by the reduction of corresponding metal salts. TiO_2 colloids (10 mM) were first prepared in ethanol by injecting controlled amount of Ti(IV) isopropoxide (Aldrich) with stirring. A solution of $HAuCl_4 \cdot 3H_2O$ or H_2PtCl_6 was mixed with a colloidal TiO_2 suspension and subjected to chemical or photochemical reduction. In the chemical reduction procedure, 10 mM solution of $NaBH_4$ in ethanol was added dropwise until a stable color is established.

Optical Measurements. Absorption spectra were recorded with a Shimadzu UV-3101 PC spectrophotometer. Transmission electron microscopy (TEM) was carried out by applying a drop of the ZnO−Au, ZnO−Pt samples to carbon-coated copper grids. Particle sizes were determined from micrographs recorded at a magnification of 150000× using a Hitachi H600 transmission electron microscope. The photoexcitation was carried out using collimated light from a 150 W xenon lamp filtered through a $CuSO_4$ solution ($\lambda > 300$ nm). Emission measurements were carried out using an SLM-S 8000 spectrofluorimeter.

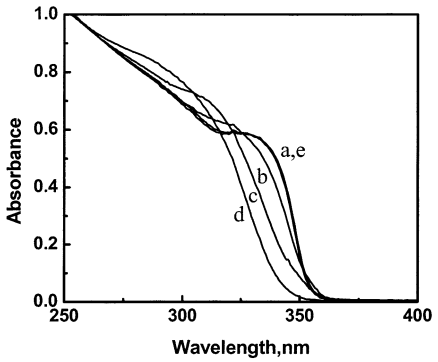

Figure 1. Absorbance spectra of 4 mM of deaerated ZnO solution in ethanol. The absorbance spectra were recorded following UV illumination for (a) $t = 0$, (b) $t = 10$, (c) $t = 20$, (d) $t = 30$ min. Spectrum e was recorded after exposing the UV-irradiated ZnO suspension to air.

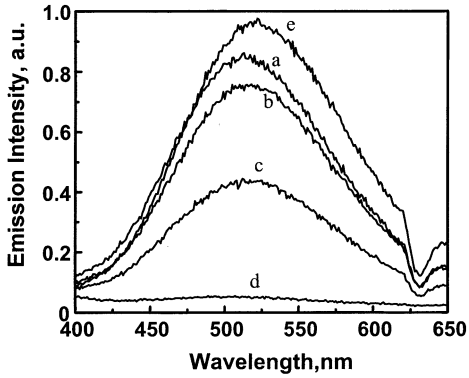

Figure 2. Emission spectra of 4 mM deaerated ZnO solution in ethanol. The spectra were recorded following UV illumination for (a) $t = 0$, (b) $t = 10$, (c) $t = 20$, (d) $t = 30$ min. Spectrum e was recorded after exposing the UV-irradiated ZnO suspension to air.

Results and Discussions

Photoinduced Electron Storage in ZnO Colloids. Freshly prepared ZnO colloidal suspensions in ethanol exhibit a strong absorption in the UV region with an onset around 330 nm. This absorption onset corresponds to a band gap of 3.76 eV, which is greater than the bulk band gap of 3.2 eV. By controlling the temperature of hydrolysis of zinc acetate precursor, it is possible to prepare various size colloids in the quantum size regime.[34] An interesting spectral feature of Q-size ZnO particles is the fact that the excitonic peak shifts to blue with decreasing particle size. During the initial period of storage (1−2 h) a growth in particle size was evident from the red-shift in the absorption edge. All the experiments were carried out after the particles were stabilized over a period of 2 h.

It has been shown earlier that electrons accumulated within the conduction band of ZnO nanostructures cause the excitonic band to bleach.[28,37] Hence this excitonic bleaching serves as a measure to estimate the electron accumulation within the ZnO nanoparticles. To study the charging events in ZnO colloids, we subjected deaerated colloidal suspensions in ethanol to UV-irradiation. The absorption and emission spectra of a 4 mM ZnO solution (deaerated by purging with N_2) recorded at different irradiation times are shown in Figures 1 and 2, respectively. As we continued the UV-irradiation for about 30 min, the excitonic band disappeared and the onset absorption shifted to blue. The role of electron storage in inducing the excitonic bleaching was further confirmed by subjecting the UV-irradiated ZnO suspension to electron scavengers. For example, a recovery of the exciton band is seen upon exposure of the UV-irradiated ZnO suspension to air. Since dissolved oxygen is a good

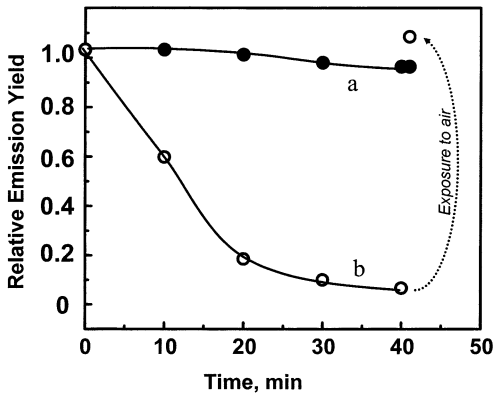

Figure 3. Effect of UV-irradiation on the emission yield of 4 mM ZnO suspension: (a) aerated, (b) deaerated by bubbling N_2. The dotted line shows the recovery of the emission following the exposure of the UV-irradiated suspension to air.

scavenger of electrons, the excess charge from ZnO nanoparticles is quickly discharged following its exposure to air.

Interestingly, ZnO emission was also found to be sensitive to charging effects during UV-irradiation. The broad emission peak of ZnO colloids at 530 nm slowly decreased as we continued the UV-irradiation. The spectrum recorded after 30 min of UV-irradiation showed negligible emission indicating thereby a complete shut-off of the radiative recombination process. Upon exposure to air the ZnO emission was restored. (The small increase in the absorbance (spectrum e) compared to the initial spectrum (spectrum a) is attributed to the possible discrepancy in oxygenation conditions and/or creation of new vacancies during UV-irradiation). Figure 3 shows the effect of UV-irradiation on the relative quantum yield of ZnO nanoparticles in deaerated and aerated solutions. Whereas no major change in the emission yield is observed in an aerated suspension, the UV-irradiation of a deaerated suspension resulted in complete quenching of the ZnO emission.

Under band gap irradiation, charge separation occurs within the ZnO nanoparticle, which is followed by the charge trapping and charge recombination processes (reactions 1 and 2):

$$\mathrm{ZnO} \rightarrow \mathrm{ZnO(e + h)} \tag{1}$$

$$\mathrm{ZnO(e)} \rightarrow \mathrm{ZnO(e_t)\ and\ ZnO(h)} \rightarrow \mathrm{ZnO(h_t)} \tag{2}$$

where e_t and h_t refer to trapped electrons and holes. The origin of the green emission in ZnO is constantly being debated and it is generally agreed that an ionizable oxygen vacancy site (V^+/V^{2+}) is responsible for the photoinduced visible emission.[39−42] Recently an effort has been made to correlate the green emissive property to the paramagnetic species V^+ in ZnO nanoparticles.[42] Under such a scenario we expect an oxygen vacancy site (V^+) to be directly involved in the radiative recombination process (reaction 3):

$$V^+ + h_{VB} \rightarrow V^{2+} + h\nu \tag{3}$$

These vacancy sites are constantly regenerated by trapping the conduction band electrons at V^{2+} sites (Reaction 4):

$$V^{2+} + e_t \rightarrow V^+ \tag{4}$$

In aerated ethanol solution, the equilibrium attained between reactions 3 and 4 and other interfacial charge transfer processes ensures the radiative charge recombination route with a low probability (<10%). The electrons and holes reaching the

SCHEME 2: Charge Separation and Charge Recombination Processes Following Bandgap Excitation of ZnO Semiconductor Nanoparticles under (a) Electron Depletion (in O_2) and (b) Accumulation (in N_2) Conditions

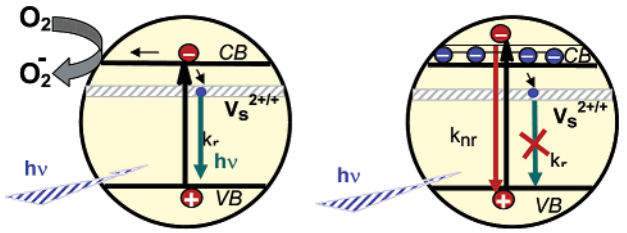

semiconductor/electrolyte are quickly scavenged by dissolved oxygen and ethanol respectively (reactions 5a & b):

$$e + O_2 \rightarrow O_2^- \tag{5a}$$

$$2h + C_2H_5OH \rightarrow CH_3^{\bullet}CHO + H^+ \tag{5b}$$

The $CH_3^{\bullet}CHO$ formed at the interface is reductive in nature and is capable of further injecting electrons into the ZnO particle. However, the fraction of the charge carriers that undergo recombination in the bulk continue to produce green emission. As long as we maintain the balance between reactions 3 and 4, and scavenging reactions at the surface (reactions 5a & 5b), we continue to observe the green emission from ZnO nanoparticles.

Once the oxygen is removed from the solution by purging N_2, photogenerated electrons fail to escape from the particles and thus accumulate within the particle. One may recall that other metal oxides such as TiO_2[43,44] and WO_3[45,46] show intense blue coloration as photogenerated electrons are accumulated in deaerated suspensions. ZnO, on the other hand, fails to exhibit such coloration effects, but it exhibits quenching of visible emission. This observation in turn shows that these accumulated electrons make the regeneration of oxygen vacancy less efficient in ZnO. The electron accumulation near the conduction band edge facilitates nonradiative charge recombination (k_{nr}) from higher energy levels. Scheme 2 illustrates the charge recombination processes under electron depletion (i.e., in the presence of O_2 or other electron scavengers) and electron accumulation (i.e., in the presence of N_2) conditions.

In semiconductor systems such as CdS and CdSe we observe a reverse phenomenon. Electron accumulation (or hole depletion) within these particles increases the emission by facilitating regeneration of traps responsible for radiative recombination. For example capping with amines has been shown to enhance the emission of CdS and CdSe colloids.[47,48] ZnO emission on the other hand is sensitive to the presence of hole scavengers. Depletion of photogenerated holes by iodide[34] or chlorinated phenols[35] results in decreased ZnO emission. The electron accumulation during the photo-irradiation of ZnO nanoparticles makes the regeneration of the oxygen vacancy less efficient. The radiative decay at these trap sites is suppressed as nonradiative electron−hole recombination becomes dominant. Since the excitation of electrons involves higher energy levels in the conduction band (see next paragraph) the rates and mode of charge recombination with valence band holes are expected to be different than those of unirradiated samples (Scheme 2).

It is important to note that the emission quenching response to charge accumulation within the ZnO nanoparticle (Figure 2) parallels the excitonic bleaching behavior observed in Figure 1. Several explanations have been invoked to explain photo-induced excitonic bleaching in semiconductor nanoparticles. These include the dynamic Burstein effect, increase in excitonic energy due to surface-trapped electrons, or Coulombic screening by photogenerated free carriers or creation of a large electric field that directly affects the excitonic levels (Stark effect) within the particles.[49−55] In the present study we attribute the shift in ZnO absorption edge during UV-irradiation to band-filling phenomenon (Moss-Burstein effect).[56,57] The fact that the absorption onset shifts to higher energy (from 360 to 340 nm during 30 min irradiation period) ascertains the accumulation of electrons near the conduction band. On the basis of the band filling model the net electron accumulation would account for filling the states of about 0.2 eV above the conduction band. These experimental observations (Figures 1 and 2) thus confirm the electron charging effects as a predominant process during UV-irradiation of ZnO nanoparticles. The electron accumulation which is achieved in the absence of electron scavengers directly influences the exciton absorption and emissive charge recombination processes.

Fluorescence Recovery Using Externally Added Electron Scavengers. To further assess the titrability of the accumulated electrons we subjected the pre-UV irradiated ZnO sample to an electron scavenger, thionine dye. Known amounts of deaerated solutions of thionine dye were added to the preirradiated ZnO suspension under nitrogen atmosphere followed by the recording of absorption and emission spectra. The dye thionine is a good electron acceptor ($E^\circ = 0.064$ versus NHE at pH 7[58]) and becomes colorless upon reduction in colloidal semiconductor suspension (reactions 6 and 7):[59]

$$\mathrm{ZnO(e)} + \mathrm{TH} \rightarrow \mathrm{ZnO} + \mathrm{TH}^{-\bullet} \quad (6)$$

$$2\mathrm{TH}^{-\bullet} \rightarrow \mathrm{TH}^{2-} + \mathrm{TH} \quad (7)$$

The one electron reduction product ($TH^{-\bullet}$) disproportionates to produce a stable two-electron reduced form of the dye, leucothionine (TH^{2-}).[59] The disappearance of the parent dye molecule (thionine) therefore corresponds to two scavengable electrons from ZnO particles ($E_{CB} = -0.5$ V versus NHE at pH 7). Figure 4 shows the difference absorption spectra recorded following each addition of thionine under deaerated conditions to both sample and reference cells. The bleaching of the absorption at 600 nm and a strong absorption in the UV (335 nm) confirm the formation of the 2-electron reduction product, leucothionine. Once all the stored electrons are titrated, no further changes could be seen in the difference absorption spectrum.

In parallel to the absorption experiments, we also recorded the emission spectrum of the UV-irradiated ZnO suspension after each addition of thionine solution. A recovery in the ZnO emission band is seen as we scavenge the electrons from the preirradiated ZnO suspension. Figure 5 compares the recovery of ZnO emission and the loss of ground-state dye absorption at 600 nm as a function of the dye concentration. The emission recovery seen in this experiment following the addition of thionine is similar to the effect of oxygen in Figure 2. The normalized traces from these spectroscopic measurements exhibit a direct relationship between the ZnO emission yield and the number of electrons stored within the particles. Furthermore, the linear dependence of the emission yield on the number of electrons scavenged from ZnO particles (inset of Figure 5) confirms a one-to-one relationship between the two

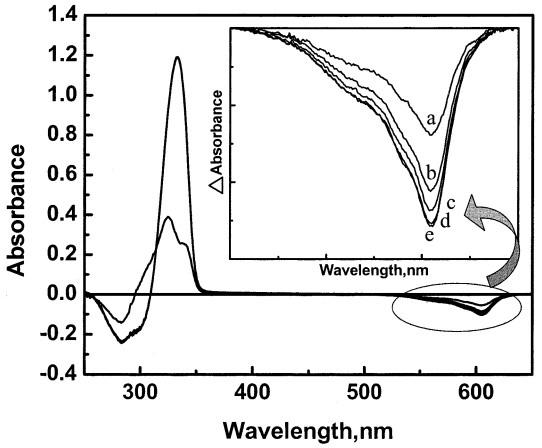

Figure 4. Difference absorption spectra of a 4 mM ZnO colloidal suspension (deaerated) after irradiation with UV-light for 30 min followed by successive addition of thionine solution (deaerated). The thionine concentrations were (a) 1.2, (b) 2.4, (c) 3.6, (d) 4.8, and (e) 6.0 μM. The inset shows the difference absorption spectra corresponding to the disappearance of the ground-state absorption of thionine as it undergoes 2 electron reduction to form leucothionine.

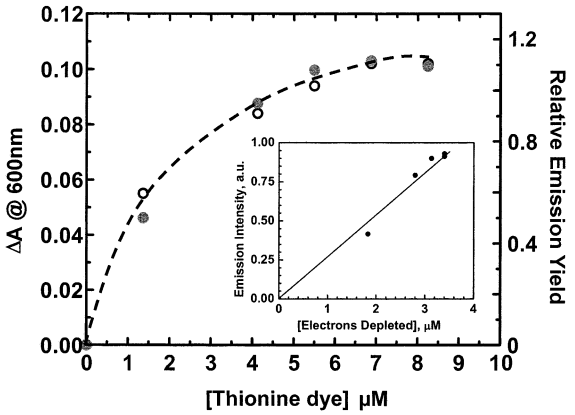

Figure 5. Dependence of (a) dyebleaching at 600 nm (○), and (b) the emission recovery (●) on the concentration of the thionine in pre UV-irradiated ZnO suspension (4 mM). Inset shows the dependence of emission intensity on the number of electrons depleted from ZnO nanoparticles. (Depletion of one thionine molecule corresponds to the scavenging of two electrons from the ZnO nanoparticle.)

independent measurements. These results further demonstrate the usefulness of ZnO emission for obtaining a quantitative estimate of electron accumulation during UV-irradiation.

Equilibration with Metal Nanoparticles. In a previous study we have shown that the semiconductor nanostructures are capable of transferring electrons to metal nanoparticles and undergo Fermi-level equilibration.[23,30] Shifting of the Fermi-level of the composite close to the conduction band edge of the semiconductor resulted in increased photopotential of the nanocomposite electrode. If, indeed, such an equilibration exists between the semiconductor−metal composite nanoparticles, we should be able to probe the charge distribution by monitoring the fluorescence recovery of the UV-irradiated ZnO system.

We tested this possibility by first irradiating deaerated ZnO colloids with UV-light until all the emission was quenched. This was followed by the addition of a deaerated gold nanoparticle suspension to the ZnO colloids. The changes in fluorescence were monitored after each addition of gold colloids. Because of the stability problems of preparing gold and platinum sols in ethanol medium, we employed TiO_2 nanoparticles as a stabilizing support.[60] In Figure 6, the emission recovery seen following the addition of metal nanoparticles is compared with

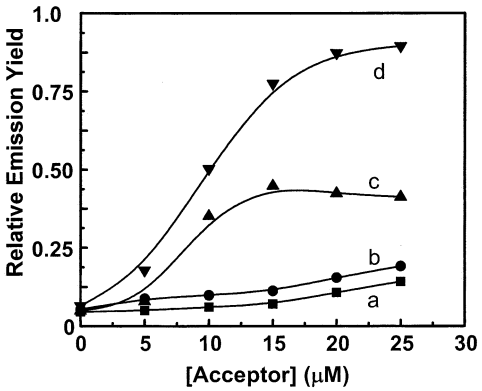

Figure 6. Recovery of the emission intensity of a deaerated ZnO solution (preirradiated with UV-light for 30 min) in the presence of various acceptors (a) ethanol, (b) TiO_2, (c) Au, and (d) Pt.

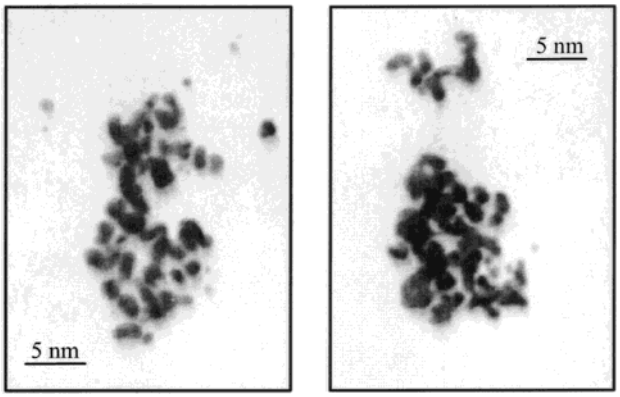

Figure 7. Transmission electron microscope (TEM) image of ZnO capped with (a) Au (left image), and (b) Pt (right image)

the corresponding blank experiments, which were carried out following the addition of ethanol and a TiO_2 colloidal suspensions (Figure 6).

Both ethanol and TiO_2 addition have little effect on the emission recovery of a pre-irradiated ZnO solution. On the other hand, the interaction with Au and Pt metal nanoparticles causes the emission to recover. While interaction with Pt colloids results in complete recovery of the ZnO emission, only about 60% recovery is seen following its interaction with gold nanoparticles. This difference in ZnO emission recovery arises from the electronic property of the corresponding metal. As shown earlier,[28] the precious metals such as Pt are ohmic in nature and facilitate discharging of electrons from the UV-irradiated ZnO nanoparticles. Au nanoparticles on the other hand have the capacity to store the electrons without facilitating their discharge into the solution. The partial emission recovery seen following the addition of gold nanoparticles suggests that a fraction of the electrons remain on ZnO nanoparticles.

Electron Storage in Metal-Capped ZnO Nanoparticles. We also employed an alternate approach of monitoring the charge distribution in semiconductor−metal composites by carrying out the metal ion reduction directly on the semiconductor surface under UV-irradiation.[28] Such a photocatalytic reduction of metal ion has been extensively employed to improve the performance of semiconductor photocatalysts.[10−12]

ZnO particles were capped with Au and Pt by reducing the corresponding metal−complex ion under UV-irradiation. The TEM images of the ZnO capped with Au and Pt are shown in Figure 7. These particles are of uniform size and spherical in shape. These particles typically are found to be in the size ranges of 50−60 Å. Because of the low concentration of metal ions

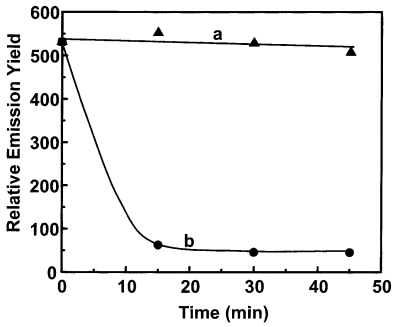

Figure 8. Emission intensity of ZnO nanoparticles (4 mM) monitored during the metal ion reduction on a ZnO surface. The ZnO suspension containing (a) 20 μM H_2PtCl_6 and (b) 20 μM $HAuCl_4$ was subjected to UV-irradiation and the emission intensity at 530 nm was monitored at different irradiation times.

TABLE 1: Kinetic Analysis of Emission Decay[a]

system	a_1	τ_1(ns)	a_2	τ_2(ns)
ZnO	5.37	3.27	1.01	31.59
ZnO@Au	4.55	3.51	0.34	31.42
ZnO@Pt	4.61	3.44	0.35	30.91

employed in these experiments ([ZnO]/[Au or Pt] = 200) we expect the overall size of these particles to be dominated mainly by the ZnO core. Note that in the absence of a ZnO core, no reduction of the metal ion could be achieved.

Figure 8 shows the decrease in ZnO emission as we carry out UV-irradiation in the presence of $AuCl_4^-$ and $PtCl_6^{2-}$ ions. Initially, the UV-irradiation causes reduction of metal−complex ions by the conduction band electrons on the ZnO surface. The reduction of the metal ion has been independently confirmed from the changes in the absorption spectra (See Supporting Information, Figure 1). As the metal islands are formed on the ZnO surface, they can either store the electrons or facilitate their discharge into the solution. In parallel to a previous set of experiments, we observe a decrease in the emission yield for the Au−ZnO system. As the photogenerated electrons get distributed between the ZnO and Au layers we observe a decrease in the emission yield. No significant changes in the emission are seen in the case of ZnO−Pt system. This again confirms the fact that the contact between ZnO and Pt remains ohmic in nature and facilitates discharge of photogenerated electrons into the solution. Because the storage of electrons within the semiconductor core becomes less favorable we do not observe any significant quenching of emission in the case of Pt-capped ZnO nanoparticles.

Emission Lifetimes. As demonstrated in earlier studies.[32,34] ZnO nanoparticles exhibit nonexponential decay and are sensitive to hole scavengers. To probe the effect of metal capping, we compared the emission decay of the ZnO, ZnO@Au, and ZnO@Pt using a 337 nm N_2 laser pulse as the excitation source. (A typical emission decay profile is shown in Supporting Information, Figure 2.) The experiments were carried out in aerated samples so that no charge accumulation occurred during UV-irradiation. The multiexponential decay curves were fitted using a nonlinear least-squares method with a two-component decay law given by eq 8:

$$F(t) = a_1 \exp(-t/\tau_1) + a_2 \exp(-t/\tau_2) \qquad (8)$$

The parameters obtained from this kinetic fit are summarized in Table 1. The short and long lifetimes that govern the decay of ZnO emission were $\tau_1 = 3.4 \pm 0.1$ ns and $\tau_2 = 31.3 \pm 0.3$ ns, respectively. The similarity of the lifetime was indicative

SCHEME 3: Photoinduced Charge Separation and Charge Distribution in (a) ZnO/Pt and (b) ZnO/Au Nanocomposites. E_F and E_f' Represent Fermi Levels Attained before and after Charge Distribution.

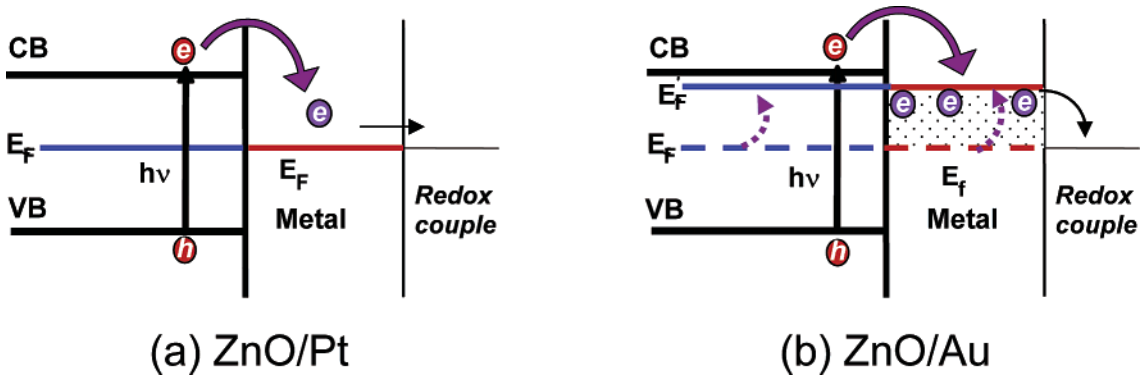

of the fact that the radiative components of the charge recombination process are not significantly affected by the presence of the metal. Whereas the decay lifetime was insensitive to the presence of the metal capping, the fraction of two decay components (a_1 and a_2 values) remained slightly different. The small decrease in the a_2 values in Table 1 indicates the dominance of the short lifetime decay component over the long-lifetime component in metal-capped ZnO nanoparticles. Such small changes in the a_1 or a_2 values can be attributed to the altered surfaces in metal-capped systems.

Fermi-Level Equilibration. On the basis of the changes in the absorption and titration of stored electrons using methyl viologen, Mulvaney and co-workers[28] found that the Fermi-level equilibration depends on the nature of the metal nanoparticles brought in contact with the irradiated semiconductor. The results presented in Figures 6 and 8 demonstrate two types of interaction between ZnO and metal (Pt and Au) systems. Scheme 3 illustrates the two types of charge distribution that can be achieved in semiconductor−metal nanocomposite systems. The interaction is ohmic type in the case of ZnO−Pt as the Pt capping merely facilitates discharge of the photogenerated electrons into the electrolyte. Such an interaction between semiconductor and metal has been proved to be beneficial for improving the efficiency of many photocatalytic reactions (for example, water splitting reactions in Pt-capped TiO_2 systems).[16,61]

The ZnO−Au system on the other hand shows unusual charge storage behavior. Whether we induce the interaction between the irradiated ZnO and Au via direct reduction of the metal ion on semiconductor surface or via addition of preformed metal nanoparticles, the photogenerated electrons get distributed between the semiconductor and metal layers. As demonstrated by electrochemical,[26,62] photochemical,[29] and spectroelectrochemical[63] experiments, gold nanoparticles possess a unique property of storing electrons. Such charge storage within the gold nanocore causes a large buildup of capacitance of the Helmoltz and diffuse double layer. As demonstrated earlier[28] the excess electron density remains mainly on the metal islands because the Helmholtz capacitance of the metal−solution interface is much higher than the space charge capacity of the semiconductor nanoparticle, even under accumulation.

The Fermi level of gold ($E_F = 0.4$ V vs NHE) is more positive than the conduction band of energy of ZnO ($E_{CB} = -0.5$ V vs NHE at pH 7). With transfer of each electron into the metal particle, the Fermi level becomes more negative. Murray and co-workers[26] have observed a shift in the energy of 0.1 V/electron for organic-capped gold nanoparticles. As the electrons get distributed between the semiconductor and metal layers they attain Fermi-level equilibration. Under these conditions, the Fermi level of the composite shifts close to the conduction band of the semiconductor. Thus, by monitoring the emission recovery one can directly probe the charge distribution between the metal and semiconductor nanoparticles.

On the basis of the titration of stored electrons using thionine, we expect storage of 8−10 electrons in a ZnO particle of 5 nm diameter. Upon equilibration with the Au nanoparticles we recover about 60% of the emission. This in turn indicates that about 40% of the initially stored electrons still remain in the ZnO particle as the two systems (viz., ZnO and Au) attain equilibration. As illustrated in Scheme 3, the electrons transferred to gold nanoparticles are stored within the metal nanocore. Increased electron density within the nanoparticle thus shift the Fermi-level toward more negative potentials. The transfer of electrons to metal nanocore continues until the Fermi level reaches close to the conduction band edge of ZnO. Each injected electron within the gold nanoparticle is capable of shifting the Fermi level by 0.1 V.[26] Thus, the storage of multiple electrons during the charge equilibration with the semiconductor can produce a significant shift in the Fermi level, thus driving the overall Fermi level to more negative potential. An independent photoelectrochemical experiment carried out with TiO_2/Au films show a shift in the Fermi-level of 150 mV.[23,30] Thus, the Fermi-level equilibration with a noble metal layer has its own benefit toward improving the photoelectrochemical and photocatalytic performance of TiO_2 systems.

Acknowledgment. The work described herein was supported by the Office of the Basic Energy Sciences of the U.S. Department of Energy. This is contribution no. NDRL 4422 from Notre Dame Radiation Laboratory.

Supporting Information Available: Two figures: (1) representing changes in absorption spectra, and (2) a typical emission decay profile. This material is available free of charge via the Internet at http://pubs.acs.org.

References and Notes

(1) Kamat, P. V. *Chem. Rev.* **1993**, *93*, 267.

(2) Rothenberger, G.; Moser, J.; Graetzel, M.; Serpone, N.; Sharma, D. K. *J. Am. Chem. Soc.* **1985**, *107*, 8054.

(3) Fendler, J. H. Photoelectron transfer in nanocomposite films, layer by layer self-assembled from polycations and anionic semiconductors. In *Semiconductor Nanoclusters—Physical, Chemical and Catalytic Aspects*; Kamat, P. V., Meisel, D., Eds.; Elsevier Science: Amsterdam, 1997; p 261.

(4) Kamat, P. V. Composite Semiconductor Nanoclusters. In *Semiconductor Nanoclusters—Physical, Chemical, and Catalytic Aspects*; Kamat, P. V., Meisel, D., Eds.; Elsevier Science: Amsterdam, 1997; p 237.

(5) Henglein, A. *J. Phys. Chem.* **1993**, *97*, 5457.

(6) Zhang, J. Z. *J. Phys. Chem. B* **2000**, *104*, 7239.

(7) Rajeshwar, K.; de Tacconi, N. R.; Chenthamarakshan, C. R. *Chem. Mater.* **2001**, *13*, 2765.
(8) Kamat, P. V. *J. Phys. Chem. B* **2002**, *106*, 7729.
(9) Kamat, P. V. *Pure Appl. Chem.* **2002**, *74*, 1693.
(10) Bard, A. J. *J. Phys. Chem.* **1982**, *86*, 172.
(11) Baba, R.; Nakabayashi, S.; Fujishima, A.; Honda, K. *J. Phys. Chem.* **1985**, *89*, 1902.
(12) Heller, A. *Pure Appl. Chem.* **1986**, *58*, 1189.
(13) Heller, A. *Nato Asi Ser., Ser. C* **1986**, *15*.
(14) Domen, K.; Sakata, Y.; Kudo, A.; Maruya, K.; Onishi, T. *Bull. Chem. Soc. Jpn.* **1988**, *61*, 359.
(15) Anpo, M.; Chiba, K.; Tomonari, M.; Coluccia, S.; Che, M.; Fox, M. A. *Bull. Chem. Soc. Jpn.* **1991**, *64*, 543.
(16) Bard, A. J.; Fox, M. A. *Acc. Chem. Res.* **1995**, *28*, 141.
(17) Nakato, Y.; Shioji, M.; Tsubomura, H. *Chem. Phys. Lett.* **1982**, *90*, 453.
(18) Hinogami, R.; Nakamura, Y.; Yae, S.; Nakato, Y. *J. Phys. Chem. B* **1998**, *102*, 974.
(19) Anpo, M.; Ichihashi, Y.; Takeuchi, M.; Yamashita, H. *Res. Chem. Intermed.* **1998**, *24*, 143.
(20) Choi, W.; Termin, A.; Hoffmann, M. R. *J. Phys. Chem.* **1994**, *98*, 13669.
(21) Zang, L.; Macyk, W.; Lange, C.; Maier, W. F.; Antonius, C.; Meissner, D.; Kisch, H. *Chem. Euro. J.* **2000**, *6*, 379.
(22) Karakitsou, K. E.; Verykios, X. E. *J. Phys. Chem.* **1993**, *97*, 1184.
(23) Subramanian, V.; Wolf, E.; Kamat, P. V. *J. Phys. Chem. B* **2001**, *105*, 11439.
(24) Nakato, Y.; Ueda, K.; Yano, H.; Tsubomura, H. *J. Phys. Chem.* **1988**, *92*, 2316.
(25) Templeton, A. C.; Wuelfing, W. P.; Murray, R. W. *Acc. Chem. Res.* **2000**, *33*, 27.
(26) Chen, S.; Ingram, R. S.; Hostetler, M. J.; Pietron, J. J.; Murray, R. W.; Schaaff, T. G.; Khoury, J. T.; Alvarez, M. M.; Whetten, R. L. *Science* **1998**, *280*, 2098.
(27) Hostetler, M. J.; Green, S. J.; Stokes, J. J.; Murray, R. W. *J. Am. Chem. Soc.* **1999**, *118*, 4212
(28) Wood, A.; Giersig, M.; Mulvaney, P. *J. Phys. Chem. B* **2001**, *105*, 8810.
(29) Ipe, B. I.; George Thomas, K.; Barazzouk, S.; Hotchandani, S.; Kamat, P. V. *J. Phys. Chem. B* **2002**, *106*, 18.
(30) Chandrasekharan, N.; Kamat, P. V. *J. Phys. Chem. B* **2000**, *104*, 10851.
(31) Koch, U.; Fojtik, A.; Weller, H.; Henglein, A. *Chem. Phys. Lett.* **1985**, *122*, 507.
(32) Bahneman, D. W.; Kormann, C.; Hoffmann, M. R. *J. Phys. Chem.* **1987**, *91*, 3789.
(33) Spanhel, L.; Anderson, M. A. *J. Am. Chem. Soc.* **1991**, *113*, 2826.
(34) Kamat, P. V.; Patrick, B. *J. Phys. Chem.* **1992**, *96*, 6829.
(35) Kamat, P. V.; Huehn, R.; Nicolaescu, R. *J. Phys. Chem. B* **2002**, *106*, 788.
(36) Chen, S. H.; Nickel, U. *J. Chem. Soc., Faraday Trans.* **1996**, *92*, 1555.
(37) Redmond, G.; O'Keeffe, A.; Burgess, C.; MacHale, C.; Fitzmaurice, D. *J. Phys. Chem.* **1993**, *97*, 11081.
(38) Hoyer, P.; Eichberger, R.; Weller, H. *Ber. Bunsen-Ges. Phys. Chem.* **1993**, *97*, 630.
(39) Butkhuzi, T. V.; Georgobiani, A. N.; Zada-Uly, Y.; El'tazarov, B. T.; Khulordava, T. V. In *Luminescence of Wideband Semiconductors*; Galanin, M. D., Ed.; Nova Science Publishers: New York, 1990; p 167.
(40) Kohan, A. F.; Ceder, G.; Morgan, D.; Walle, C. G. V. d. *Phys. Rev. B* **2000**, *61*, 15019.
(41) Leiter, F. H.; Alves, H. R.; Hofstaetter, A.; Hofmann, D. M.; Meyer, B. K. *Phys. Status Solidi B−Basic Research* **2001**, *226*, R4.
(42) Vanheusden, K.; Warren, W. L.; Seager, C. H.; Tallant, D. R.; Voigt, J. A.; Gnade, B. E. *J. Appl. Phys.* **1996**, *79*, 7983.
(43) Bedja, I.; Hotchandani, S.; Kamat, P. V. *J. Phys. Chem.* **1993**, *97*, 11064.
(44) Hotchandani, S.; Bedja, I.; Fessenden, R. W.; Kamat, P. V. *Langmuir* **1994**, *10*, 17.
(45) Kamat, P. V.; Bedja, I.; Hotchandani, S. *J. Phys. Chem.* **1994**, *98*, 9137.
(46) Dawson, A.; Kamat, P. V. A simple photocatalytic experiment to generate fullerene anions. In *Fullerenes 2000: Chemistry and Physics of Fullerenes and Carbon Nanoclusters*; Kamat, P. V., Guldi, D. M., Kadish, K. M., Eds.; The Electrochemical Society: Pennington, 2000; Vol. 10, p 34.
(47) Kamat, P. V.; de Lind, M.; Hotchandani, S. *Isr. J. Chem.* **1993**, *33*, 47.
(48) Chandrasekharan, N.; Kamat, P. V. *Res. Chem. Intermed.* **2002**, *28*, 847.
(49) Haase, M.; Weller, H.; Henglein, A. *J. Phys. Chem.* **1988**, *92*, 4706.
(50) Henglein, A.; Kumar, A.; Janata, E.; Weller, H. *Chem. Phys. Lett.* **1986**, *132*, 133.
(51) Banyai, L.; Koch, S. W. *Phys. Rev. Lett.* **1986**, *57*, 2722.
(52) Liu, C.; Bard, A. J. *J. Phys. Chem.* **1989**, *93*, 3232.
(53) Kamat, P. V.; Dimitrijevic, N. M.; Nozik, A. J. *J. Phys. Chem.* **1989**, *93*, 2873.
(54) Hilinski, E. F.; Lucas, P. A.; Wang, Y. *J. Chem. Phys.* **1988**, *89*, 3435.
(55) Wang, Y.; Suna, A.; McHugh, J.; Hilinski, E. F.; Lucas, P. A.; Johnson, R. D. *J. Chem. Phys.* **1990**, *92*, 6927.
(56) Moss, T. S. *Proc. Phys. Soc. (London) B* **1954**, *67*, 775.
(57) Burstein, B. E. *Phys. Rev.* **1954**, *93*, 632.
(58) Clark, W. M. *Oxidation−Reduction Potentials of Organic Systems*; The Williams & Wilkins Co.: Baltimore, 1960.
(59) Kamat, P. V. *J. Photochem.* **1985**, *28*, 513.
(60) Since we cap the TiO_2 core with a metal layer, we expect the role of TiO_2 to be quite passive. Independent experiments carried out with TiO_2 colloids did not exhibit any noticeable changes on the spectral properties of ZnO.
(61) Ashokkumar, M. *Int. J. Hydrogen Energy* **1998**, *23*, 427.
(62) Chen, S.; Murray, R. W. *J. Phys. Chem. B* **1999**, *103*, 9996
(63) Kamat, P. V.; Barazzouk, S.; Hotchandani, S. *Angew. Chem. (Int. Ed.)* **2002**, *41*, 2764.